

RESEARCH

Open Access



Genetic labeling reveals spatial and cellular expression pattern of neuregulin 1 in mouse brain

Chen-Yun Ding^{1,2†}, Yan-Ting Ding^{1†}, Haifeng Ji^{1,3}, Yao-Yi Wang¹, Xinwen Zhang^{2,4*} and Dong-Min Yin^{1,5*} 

Abstract

Background Where the gene is expressed determines the function of the gene. Neuregulin 1 (Nrg1) encodes a tropic factor and is genetically linked with several neuropsychiatry diseases such as schizophrenia, bipolar disorder and depression. Nrg1 has broad functions ranging from regulating neurodevelopment to neurotransmission in the nervous system. However, the expression pattern of Nrg1 at the cellular and circuit levels in rodent brain is not fully addressed.

Methods Here we used CRISPR/Cas9 techniques to generate a knockin mouse line (Nrg1^{Cre/+}) that expresses a P2A-Cre cassette right before the stop codon of Nrg1 gene. Since Cre recombinase and Nrg1 are expressed in the same types of cells in Nrg1^{Cre/+} mice, the Nrg1 expression pattern can be revealed through the Cre-reporting mice or adeno-associated virus (AAV) that express fluorescent proteins in a Cre-dependent way. Using unbiased stereology and fluorescence imaging, the cellular expression pattern of Nrg1 and axon projections of Nrg1-positive neurons were investigated.

Results In the olfactory bulb (OB), Nrg1 is expressed in GABAergic interneurons including periglomerular (PG) and granule cells. In the cerebral cortex, Nrg1 is mainly expressed in the pyramidal neurons of superficial layers that mediate intercortical communications. In the striatum, Nrg1 is highly expressed in the Drd1-positive medium spiny neurons (MSNs) in the shell of nucleus accumbens (NAc) that project to substantia nigra pars reticulata (SNr). In the hippocampus, Nrg1 is mainly expressed in granule neurons in the dentate gyrus and pyramidal neurons in the subiculum. The Nrg1-expressing neurons in the subiculum project to retrosplenial granular cortex (RSG) and mammillary nucleus (MM). Nrg1 is highly expressed in the median eminence (ME) of hypothalamus and Purkinje cells in the cerebellum.

Conclusions Nrg1 is broadly expressed in mouse brain, mainly in neurons, but has unique expression patterns in different brain regions.

Keywords Neuregulin 1, Cre-reporting mice, Olfactory bulb, Striatum, Cerebral cortex, Hippocampus, Hypothalamus, cerebellum, axon projection

[†]Chen-Yun Ding and Yan-Ting Ding have contributed equally to this work

*Correspondence:

Xinwen Zhang
zhangxinwen@cmu.edu.cn

Dong-Min Yin
dmyin@brain.ecnu.edu.cn

Full list of author information is available at the end of the article



Background

Neuregulin 1 (Nrg1) encodes a tropic factor and is genetically associated with several neuropsychiatric diseases such as schizophrenia, bipolar disorder and depression [1–4]. NRG1 also shows neuroprotective effects in animal models of some neurological disorders such as ischemic stroke, epilepsy and Alzheimer's disease [5–8]. NRG1 is a transmembrane protein and includes the N-terminal extracellular domain (ECD) and the C-terminal intracellular domain (ICD) [9]. The ECD of NRG1 binds with ErbB3 and ErbB4 receptors and activates the downstream signaling pathway. The NRG1-ErbB signaling is important for neurodevelopment such as myelination and GABAergic circuit formation [10–13]. NRG1-ErbB signaling also regulates synaptic transmission and plasticity such as GABA release and long-term potentiation (LTP) [14–18]. The ICD of NRG1 interacts with LIM kinase 1 (LIMK1) and sodium channel Nav1.1 to regulate glutamatergic transmission and neuronal excitability, respectively [19–22]. In addition, the ICD of NRG1 can bind with the gene promoter to regulate gene transcription [23–25].

Nrg1 mRNA has different splicing isoforms, each with a distinct N-terminal region. At least 6 types of splicing isoforms of Nrg1 mRNA were expressed throughout the brain [26]. Nrg1 is highly expressed in neurons in the mammalian brain [14, 27–29] although some studies reported Nrg1 was also expressed in glia cells [26, 27]. In the cerebral cortex and hippocampus, Nrg1 is mainly expressed in excitatory pyramidal neurons [6, 10, 27] while the ErbB4 receptor is specifically expressed by GABAergic interneurons [12, 30, 31].

The current knowledge about the function of NRG1 is mainly from the experiments with purified NRG1-ECD or ICD. The functions of endogenous Nrg1 and the Nrg1-expressing neurons are relatively unexplored [32, 33]. A prerequisite for addressing these issues is to understand the cellular expression pattern of Nrg1 and the axon projections of Nrg1-expressing neurons, i.e. expression pattern of Nrg1 at the cellular and circuit levels. The previous studies on the cellular expression pattern of Nrg1 include those from *in situ* hybridization (ISH), immunohistochemistry and translating ribosome affinity purification (TRAP) [14, 27, 28, 34]. However, the results from previous studies were sometimes controversial and did not reveal the expression pattern of Nrg1 at the circuit level.

The recently developed techniques of genetic labeling have enabled clear visualization of gene expression at the cellular level. These techniques usually include the use of a knockin mouse line which expresses the Cre recombinase immediately before the stop codon of the gene of interest, and a reporting mouse line which express

fluorescent proteins in a Cre-dependent manner [31, 35–37]. Here we used CRISPR/Cas9 techniques to generate Nrg1^{Cre/+} knockin mice which express the Cre recombinase immediately before the stop codon of Nrg1 gene. By crossing the Nrg1^{Cre/+} mice with the Cre-dependent reporting mice (Ai14) [35], we generated the Nrg1-reporting mice which express tdTomato in Nrg1-positive cells. We then analyzed the cellular expression pattern of Nrg1 in the brain of Nrg1-reporting mice. We further injected Cre-dependent reporting AAV into the brain regions of adult Nrg1^{Cre/+} mice. Through this approach, we explored Nrg1 expression pattern and the axon projections of Nrg1-positive neurons in adult mouse brain. These results provide a fundamental framework for the study of Nrg1 function in the rodent brain. Moreover, the Nrg1^{Cre/+} mice generated here may represent a useful tool to study the function of neuronal populations expressing Nrg1.

Methods

Generation of Nrg1^{Cre/+} knockin mice

A P2A-Cre cassette was placed between the coding sequence of axon 9 (immediately before the stop codon) and the 3' UTR of mouse Nrg1 gene (Fig. 1A). The P2A is a small peptide originally from porcine teschovirus and can be self-cleaved at its C terminus in all eukaryotic cells [38]. In the Nrg1^{Cre/+} knockin mice, a fusion protein NRG1-P2A-Cre are transiently expressed but NRG1 and Cre proteins are ultimately separated after P2A-mediated cleavage. The detail of using CRISPR/Cas9 techniques to do gene editing in mice was described previously [39]. Briefly, sgRNA, Cas9 mRNA, and targeting vectors were injected into the cytoplasm of one-cell stage embryos through the injection needle. Injections were performed using an Eppendorf transferMan NK2 micromanipulator. Injected zygotes were transferred into pseudopregnant female C57BL/6 mice after 2-h culture in KSOM medium. This strain was generated in Beijing Biocytogen Co., Ltd., and maintained on a C57BL/6 background. The F0 chimera mice were crossed with wild type (WT) mice to get the germline transmission F1 mice. The correct targeting of the Nrg1^{Cre/+} in F1 mice was confirmed by southern blot and gene sequencing. The primers for genotyping the WT-Nrg1 and Nrg1::Cre allele are as follows: forward: 5'atggccacattgccaataggttga3'; reverse: 5'tgctctcgacataacataaagga3'. The PCR products for WT-Nrg1 and Nrg1::Cre alleles were 514 and 1633 bp, respectively.

Generation of Nrg1-reporting mice

The F1 Nrg1^{Cre/+} mice were backcrossed with WT mice to get the F2 Nrg1Cre/+ mice. The F2 Nrg1^{Cre/+} mice were crossed with heterozygous Ai14 mice

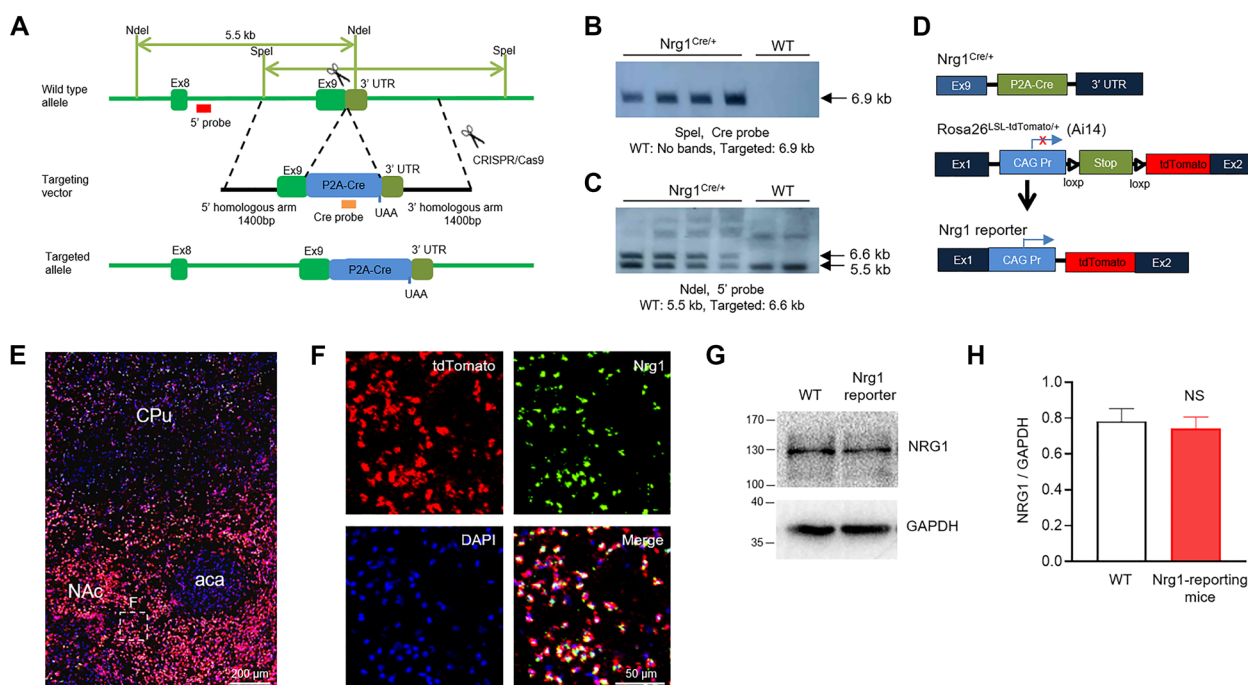


Fig. 1 Generation and validation of *Nrg1*-reporting mice. **A** Schematic diagram of the gene targeting strategy to insert the P2A-Cre cassette immediately before the stop codon of the *Nrg1* locus, between exon 9 and 3' untranslated region (3'UTR). The p2A peptide will be cleaved and two independent protein NRG1 and CRE will be expressed. **B** Southern blot screen for *Nrg1*^{Cre/+} mice using SpeI-digested genomic DNA and the Cre probe indicated in panel A. The targeted *Nrg1* allele will yield a DNA fragment of 6.9 kb. **C** Southern blot screen for *Nrg1*^{Cre/+} mice using NdeI-digested genomic DNA and the 5' probe indicated in panel A. The wild-type and targeted *Nrg1* allele will yield a DNA fragment of 5.5 kb and 6.6 kb, respectively. **D** The breeding strategy to get the *Nrg1*-reporting mice. The female *Nrg1*^{Cre/+} mice were crossed with the male *Rosa26*^{LSL-tdTomato/+} (*Ai14*) mice to get the *Nrg1*^{Cre/+}; *Rosa26*^{LSL-tdTomato/+} mice, i.e., the *Nrg1*-reporting mice. **E** Double fluorescence in situ hybridization (dFISH) of tdTomato and *Nrg1* mRNA in the striatum of *Nrg1*-reporting mice. The arrows indicate *Nrg1*-positive granule cells in the OB. Scale bar, 200 μ m. **F** The enlarged image from the rectangle in panel E. Scale bar, 50 μ m. **G–H** Similar NRG1 protein levels in the striatum between WT and *Nrg1*-reporting mice. G, representative western blots, the total lysates of striatum from WT and *Nrg1*-reporting mice were probed with anti-NRG1 and anti-GAPDH antibodies. H, quantification results. NS, not significant, $n = 3$, unpaired t-test

(*Rosa26*^{LSL-tdTomato/+} mice, JAX stock #007908) [35] to get the *Nrg1*^{Cre/+}; *Rosa26*^{LSL-tdTomato/+} mice (abbreviated to *Nrg1*-reporting mice). The tdTomato was specifically expressed in the cells with Cre activity which was controlled by the *Nrg1* promoter. Cre dependent expression of tdTomato has frequently been used to study the expression pattern of genes with a high temporal and spatial resolution [31, 35–37]. Mice were housed at 23 °C with a 12 h light/dark cycle and food and water available ad libitum. Both female and male *Nrg1*-reporting mice were used and showed similar *Nrg1* expression pattern in forebrain regions. For the quantification, at least three different mice were used for each group. The *Nrg1*-reporting mice were crossed with *Gad67*-GFP mice [40] to visualize *Nrg1* expression in GABAergic interneurons. All experimental procedures were reviewed and approved by the institutional animal care and use committee of East China Normal University.

Fluorescence in situ hybridization (FISH)

FISH for mRNA expression was performed manually using the RNAscope Multiplex Fluorescent Reagent Kit v2 (Advanced Cell Diagnostics, Inc., Hayward, CA, USA) following the manufacturer's instruction. The RNAscope probes targeting *Nrg1*, tdTomato and *Drd1* were from Advanced Cell Diagnostics. The reference numbers are as follows: 418181-C3 for *Nrg1* probe, 317041 for tdTomato probe, 406491 for *Drd1* probe.

Immunofluorescence

After being anesthetized with euthatal (from Merck) (60 mg/kg), the *Nrg1*-reporting mice (2 months old) were transcardially perfused with PBS (2 ml/g of body weight), followed by 4% PFA in PBS. Brains were harvested, incubated in 4% PFA overnight, and dehydrated at 4 °C in two steps with 20% and 30% sucrose in PBS. Brains were frozen in OCT (catalog #14-373-65; Fisher) and sectioned into 40 μ m slices on a cryostat microtome

(Bosch Microm HM550) at -20°C . Brain slices were permeabilized with 0.3% TritonX 100 and 5% BSA in PBS and incubated with primary antibodies at 4°C overnight. The brain slices were not treated with Triton- \times 100 when staining with anti-GAD67 antibodies. After washing with PBS for three times, samples were incubated with Alexa Fluor-488 or -647 secondary antibodies (1:1000, ThermoFisher Scientific) for 1 h at room temperature. Samples were mounted with Vectashield mounting medium (Vector) and images were taken by Leica TCS SP8 confocal microscope. The following primary antibodies were used: rabbit anti-NeuN (1:500, Abcam, ab177487), rabbit anti-TH (1:250, Millipore, MAB152), mouse anti-NRGN (1:200, R&D, MAB7947), mouse anti-PV (1:500, Sigma, P3088), mouse anti-GFAP (1:250, Millipore, MAB360); rabbit anti-S100 β (1:200, Abcam, Ab52642) and mouse anti-GABA (1:1000, Invitrogen, PA5-32241).

Analysis of Nrg1-positive cells in brain slices

Images were taken on a Leica TCS SP8 scanning confocal microscopy. Unbiased stereology (Tissue Gnostics, Vienna, Austria) was applied to quantification of Nrg1⁺ cell number in brain slices [36, 37]. The detailed methods for cell number counting is available on the website (<https://tissuegnostics.com/products/single-cell-analysis/tissuequest>). To compare the Nrg1 expression among different brain regions of adult mice, we count the density of Nrg1⁺ cells. The density was calculated from eight continuous sections in Z-stack. Coronal brain slices from 4.3 to 3.9 mm relative to bregma were used to study OB, 1.7 to 1.4 mm relative to bregma were used to access striatum, -1.5 – -1.8 mm relative to bregma were used to study primary somatosensory cortex (SS1), -1.7 – -1.9 mm relative to bregma were used to investigate dorsal hippocampus.

Western blot

Homogenates of striatum from WT and Nrg1-reporting mice were prepared in RIPA buffer containing 50 mM Tris-HCl, pH 7.4, 150 mM NaCl, 2 mM EDTA, 1% sodium deoxycholate, 1% SDS, 1 mM PMSE, 50 mM sodium fluoride, 1 mM sodium vanadate, 1 mM DTT, and protease inhibitors cocktails. Homogenates were resolved on SDS/PAGE and transferred to nitrocellulose membranes, which were incubated in the TBS buffer containing 0.1% Tween-20 and 5% milk for 1 h at room temperature before the addition of primary antibody for incubation overnight at 4°C . After wash, the membranes were incubated with HRP-conjugated secondary antibody in the same TBS buffer for 1 h at room temperature. Immunoreactive bands were visualized by ChemiDoc™ XRS+ Imaging System (BIO-RAD) using enhanced chemiluminescence (Pierce) and analyzed with Image J

(NIH). The following antibodies were used: rabbit anti-NRG1 (1:1000, Cell Signaling Technology, #2573) and mouse anti-GAPDH (1:8000, Arigo, ARG10112).

Stereotaxic injection of AAV into brain regions

The Cre-reporting AAV (pAAV-EF1 α -loxp-stop-loxp-tdTomato-WPRE-polyA, titer 1×10^{13} / μl) was generated by Obio Technology (Shanghai) Corp., Ltd. Adult Nrg1^{Cre/+} mice (2-month-old) were anesthetized with euthatal (60 mg/kg, i.p. injection) and headfixed in a stereotaxic device (RWD life science). Each injection used 0.5 μl AAV and took 10 min. After injection, the glass pipette was left in place for 10 min to facilitate diffusion of the virus. The injection sites were examined at the end of the experiments, and animals with incorrect injection site were excluded from the data analysis. Injection coordinates are as follows: anteroposterior (AP) 3.92 mm, dorsoventral (DV) 1.75 mm, mediolateral (ML) 0.75 mm relative to bregma for olfactory bulb; AP -1.82 mm, DV 1.90 mm, and ML 1.12 mm relative to bregma for dentate gyrus; AP+1.42 mm, DV 5.00 mm, and ML 1.15 mm relative to bregma for striatum; AP -6.24 mm, DV 2.00 mm, and ML 0 mm relative to bregma for cerebellum. Four weeks after AAV injection, mice were subjected to experiments. All surgery was conducted with aseptic technique.

Statistics

All the data were shown as mean \pm SEM. Comparisons between two groups were made using unpaired t test. Comparisons between three or more groups were made using one-way ANOVA analysis followed by Tukey's post hoc test. Analysis of the data from different layers of multiple cortical regions were performed using two-way-ANOVA followed by Tukey's multiple comparison test. The p values were provided in the figure legends and were significant when smaller than 0.05. The statistical analysis was performed with the software of GraphPad Prism 8.

Results

Generation and validation of Nrg1-reporting mice

We first generated Nrg1^{Cre/+} knockin mice where a P2A-Cre cassette was placed right before the stop codon (UAA) of Nrg1 gene (Fig. 1A) (see details in the Method). In the Nrg1^{Cre/+} knockin mice, the expression of Cre is under the control of endogenous Nrg1 promoter and thus Cre and Nrg1 are expressed in the same types of cells. The results from Southern blot validated the insertion of P2A-Cre into the target locus, indicating that the generation of Nrg1^{Cre/+} mouse line is methodologically reliable (Fig. 1B, C). To acquire the Nrg1-reporting mice, the Nrg1^{Cre/+} mice were crossed

with the Cre-reporting Ai14 mice [35] (Fig. 1D). The *Nrg1*-reporting mice develop normally and are fertile. To verify that tdTomato is specifically and faithfully expressed in *Nrg1*-positive cells from *Nrg1*-reporting mice, we performed FISH to detect the *Nrg1* mRNA in the nucleus accumbens (NAc) where the expression of *Nrg1* is high [41]. As shown in Fig. 1E, F, *Nrg1* mRNA was well colocalized with tdTomato in the NAc of *Nrg1*-reporting mice. Most tdTomato-positive cells ($94 \pm 1.2\%$) in the NAc of *Nrg1*-reporting mice express *Nrg1* mRNA. In addition, the protein levels of NRG1 in the striatum are similar between the *Nrg1*-reporting mice and their wild type (WT) littermates (Fig. 1G, H). Thus, we validated on mRNA levels that tdTomato from *Nrg1*-reporting mice can be used as a faithful indicator of *Nrg1*-positive cells.

Expression pattern of *Nrg1* in the olfactory bulb

We analyzed the densities of *Nrg1*-positive cells in several brain regions of *Nrg1*-reporting mice, and revealed that the olfactory bulb (OB) had the most abundant *Nrg1*-positive cells (Additional file 1: Fig. S1). The OB is the first brain region where olfactory information is processed. The OB can be divided into olfactory nerve layer (ONL), glomerular layer (GL), external plexiform layer (EPL), mitral layer (ML), internal plexiform layer (IPL) and granular cell layer (GCL) (Fig. 2A, B). The *Nrg1*-positive cells were most abundant in the GCL, accounting for $73.4 \pm 2.3\%$ of the total *Nrg1*-positive cells, followed by the ML and GL, accounting for $23.6 \pm 3.0\%$ and $7.27 \pm 2.8\%$ of the total *Nrg1*-positive cells, respectively (Fig. 2B, C). *Nrg1* is also highly expressed in the granule cell layer of the accessory olfactory bulb (GrA) (Fig. 2B).

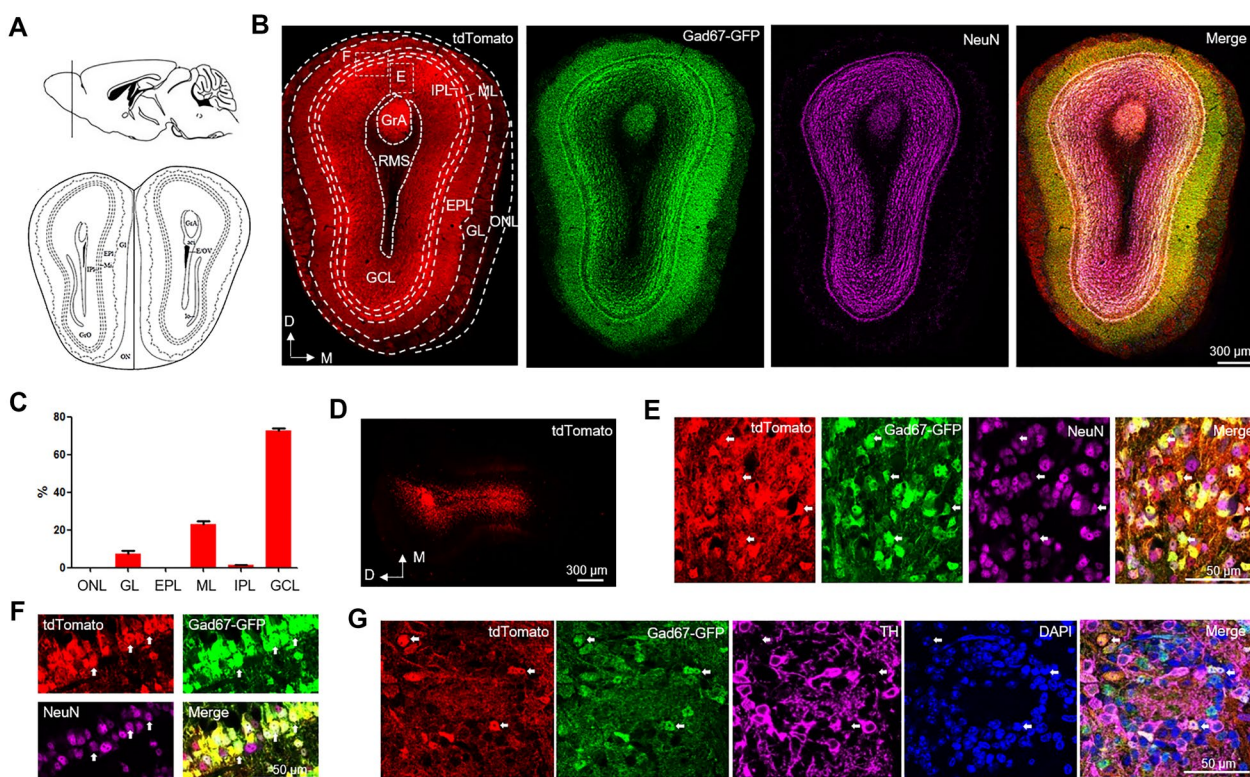


Fig. 2 Expression pattern of *Nrg1* in the olfactory bulb. **A** Diagram of mouse brain sagittal section (top) and coronal section (bottom). The line in the sagittal section diagram indicates the position of the coronal section. **B** Fluorescent images of tdTomato, Gad67-GFP and NeuN in the OB of 2-month-old *Nrg1*-reporting mice. D, dorsal. M, medial. Scale bar, 300 μ m. **C** The percentage of *Nrg1*-positive cells in different layers among total *Nrg1*-positive cells in the OB. $P < 0.0001$, $n = 3$ mice (9 slices), one-way-ANOVA. **D** Expression of tdTomato after injection of Cre-reporting AAV into the GCL of 2-month-old *Nrg1*^{Cre/+} mice. Four weeks after AAV injection, the brain slices were collected and analyzed. Scale bar, 300 μ m. **E** Fluorescent images of tdTomato, Gad67-GFP and NeuN in the GCL, from the rectangle E in panel B. Arrows indicate *Nrg1*-positive granular cells in the GCL. Scale bar, 50 μ m. **F** Fluorescent images of tdTomato, Gad67-GFP and NeuN in the ML, from the rectangle F in panel B. Arrows indicate *Nrg1*-positive GABAergic interneurons in the ML. Scale bar, 50 μ m. **G** Fluorescent images of tdTomato, Gad67-GFP, TH and DAPI in GL. Arrows indicate *Nrg1*-positive PG cells expressing Gad67-GFP but not TH. Scale bar, 50 μ m. The *Nrg1*-reporting mice were crossed with Gad67-GFP mice to visualize the expression of *Nrg1* in GABAergic interneurons. ONL: olfactory nerve layer; GL: glomerular layer; EPL: external plexiform layer; ML: mitral cell layer; IPL: internal plexiform layer; GCL: granular cell layer; GrA: granule cell layer of the accessory olfactory bulb; RMS: rostral migratory stream

However, few *Nrg1*-positive cells are distributed in ONL, EPL, IPL and rostral migratory stream (RMS) (Fig. 2B, C). Adult expression of *Nrg1* in the GCL of OB has not been well reported, which raises the possibility that the tdTomato signal we observed may arise from the transient expression of *Nrg1* in the early development instead of in the adulthood. To address this possibility, we injected Cre-reporting AAV into the GCL of 2-month-old WT and *Nrg1*^{Cre/+} mice. After injecting AAV into the GCL of WT mice, tdTomato did not appear in granule cells (data not shown). However, when AAV was injected into the GCL of *Nrg1*^{Cre/+} mouse, the expression of tdTomato was observed in granule cells (Fig. 2D). These results indicated that *Nrg1* is, indeed, expressed in the granule cells of OB in adult mice.

We crossed the *Nrg1*-reporting mice with Gad67-GFP mice to investigate whether *Nrg1* is expressed in the GABAergic interneurons. In the GCL and ML, *Nrg1* is expressed in the GABAergic interneurons as indicated by the co-localization of tdTomato and GFP (Fig. 2E, F). In the GL, *Nrg1* is expressed in the periglomerular (PG) cells that are GABAergic interneurons as evidenced by the co-localization of tdTomato with GFP (Fig. 2G). In contrast, tdTomato was not co-localized with tyrosine hydroxylase (TH, a protein marker for short-axon cells in the GL), which suggests that *Nrg1* is not expressed in short-axon cells in the GL (Fig. 2G). Together, these results demonstrate that *Nrg1* is mainly expressed in GABAergic interneurons in mouse OB.

Expression pattern of *Nrg1* in the cerebral cortex

The cerebral cortex is the outer most structure of the mammalian brain having a distinct six-layer composition. Here, high-level processing occurs for many processes including motor control, sensory perception, attention, and memory. *Nrg1*-positive cells were widely distributed in different cortical regions. The density of *Nrg1*-positive cells is relatively higher in the cingulate cortex, area 1 (Cg1), retrosplenial cortex (RS), piriform cortex (Pir) and auditory cortex (Au) than that in the primary motor cortex (M1), secondary motor cortex (M2), primary somatosensory cortex (SS1), secondary somatosensory cortex (SS2) and lateral entorhinal cortex (LE) (Fig. 3A). *Nrg1* was expressed in different layers of cerebral cortex. However, the percentage of *Nrg1*-positive cells in the superficial layers is significantly higher than deep layers in multiple cortical regions (Fig. 3B). In the following study, we take the cortical region of SS1 as an example.

In the SS1, tdTomato signal was mainly distributed in the superficially layer 2–3 (Fig. 3D, E). The tdTomato signal was localized in some fiber-like structure and cell bodies that express NeuN (a pan neuronal marker) and neurogranin (NRGN, a pyramidal neuronal marker), but

not all NRGN-positive cells expressed *Nrg1* (3E and 3F). We further crossed the *Nrg1*-reporting mice with Gad67-GFP mice to investigate whether *Nrg1* is expressed in the GABAergic interneurons in the SS1. As shown in Fig. 3G, we did not observe the co-expression of tdTomato and GFP in the same cells, indicating low expression of *Nrg1* in GABAergic interneurons in the SS1. Overall these data suggest that *Nrg1* is mainly expressed in part of pyramidal neurons in the superficial layers of SS1.

Expression pattern of *Nrg1* in the striatum

Apart from locomotion, the striatum has been closely implicated in regulating reward and motivation. The dorsal and ventral part of striatum are composed of the caudate putamen (CPu) and NAc, respectively. Most neurons in the striatum are GABAergic medium spiny neurons (MSNs) which receive dopaminergic input from substantia nigra (SN) and ventral tegmental area (VTA). In the striatum, *Nrg1*-positive cells were mainly distributed in the regions of ventral striatum including the shell of NAc (AcbSH) and olfactory tubercle (Tu) (Fig. 4A–D). By contrast, the *Nrg1*-positive cells are quite sparse in the core of NAc (AcbC) and CPu (Fig. 4B, D).

We crossed *Nrg1*-reporting mice with Gad67-GFP transgene mice to verify whether *Nrg1* is expressed in the GABAergic MSNs in the striatum. All *Nrg1*-positive cells in the Tu and AcbSH are GABAergic MSNs but not vice versa because all the tdTomato-positive cells express GFP while only some of the GFP-positive cells express tdTomato (Fig. 4C, D). One type of MSNs express dopamine D1 receptor (*Drd1*) and directly project to substantia nigra pars reticulata (SNr), which is called the direct pathway [42]. The other type of MSNs express dopamine D2 receptor (*Drd2*) and connect with SNr indirectly through external globus pallidus (GPe) and subthalamic nucleus, which is referred to indirect pathway [42]. Intriguingly, we found strong expression of axon fiber-like tdTomato signal in the SNr (Fig. 4E), which suggest that *Nrg1*-positive cells in the NAc have axon projections to the SNr. To verify this hypothesis, we performed stereotaxic injection of Cre-reporting AAV into the NAc of 2-month-old *Nrg1*^{Cre/+} mice. Four weeks after AAV injection, we found tdTomato-positive cells in the NAc and tdTomato-positive axon fibers in the SNr (Fig. 4F, G). These results indicate that *Nrg1*-positive cells directly send their axons to SNr, i.e., *Nrg1* is expressed in the MSNs of the direct pathway. We further performed FISH to investigate whether *Nrg1* and *Drd1* (a maker for the MSNs in the direct pathway) are expressed in the same type of cells. This is indeed the case because most *Nrg1*-positive cells also expressed *Drd1* (Fig. 4H and 4I).

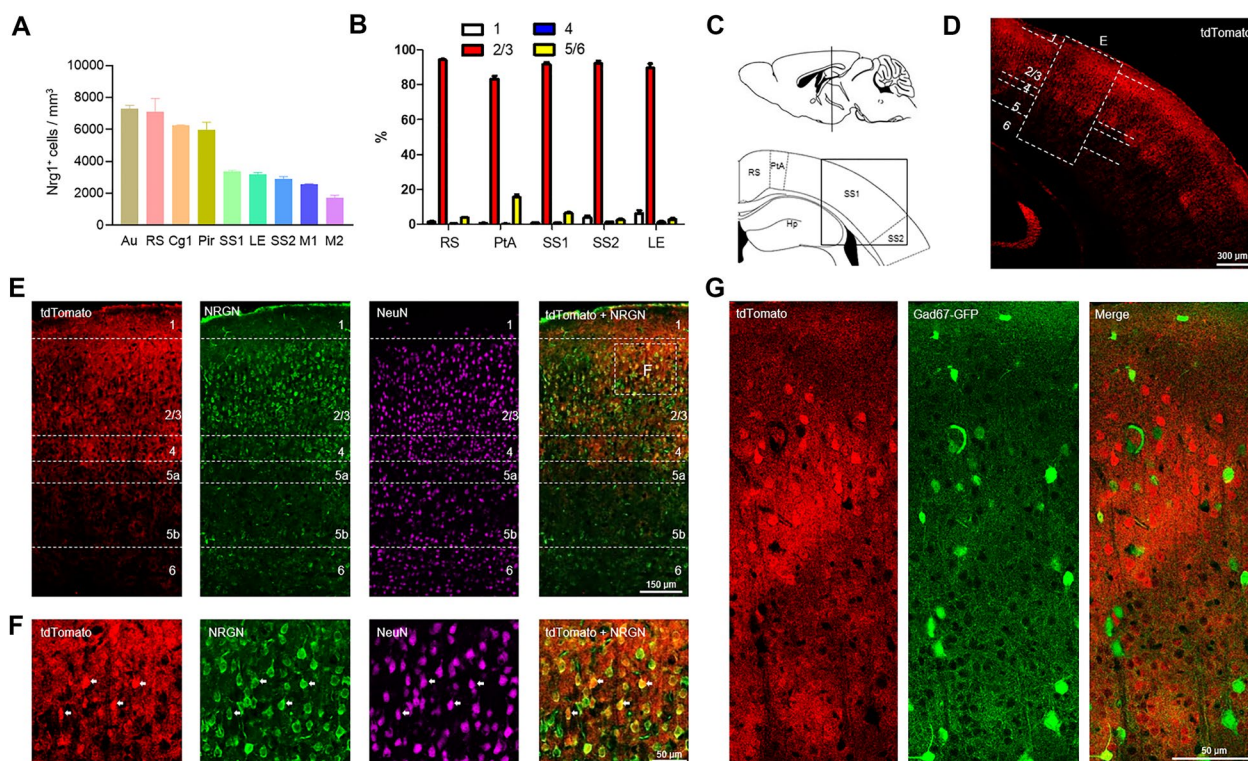


Fig. 3 Expression pattern of *Nrg1* in the cerebral cortex. **A** The densities of *Nrg1*-positive cells in different regions of cerebral cortex from 2-month-old *Nrg1*-reporting mice. $P < 0.0001$, $n = 3$ mice (6 slices) for Au and LE, $n = 3$ mice (9 slices) for other cortical regions, one-way-ANOVA. **B** The percentage of *Nrg1*-positive cells in different layers among total *Nrg1*-positive cells from multiple cortical regions. Layer factor $P < 0.0001$, region factor $P > 0.99$, $n = 3$ mice (9 slices) for each cortical region, two-way-ANOVA. **C** Diagram of mouse brain sagittal section (top) and coronal section (bottom). The line in the sagittal section diagram indicates the position of the coronal section. The rectangle indicates the brain region shown in panel D. **D** Fluorescent images of tdTomato in the SS1. Scale bar, 300 μm . **E** Fluorescent images of tdTomato, NRGN and NeuN, from the rectangle in panel D. Scale bar, 150 μm . **F** Fluorescent images of tdTomato, NRGN and NeuN, enlarged from the rectangle in panel E. Arrows indicate *Nrg1*-positive pyramidal neurons. Scale bar, 50 μm . **G** Fluorescent images of tdTomato and gad67-GFP in the SS1. Scale bar, 50 μm . Au: auditory cortex; RS: retrosplenial cortex; Cg1: cingulate cortex, area 1; Pir: piriform cortex; SS1: primary somatosensory cortex; LE: lateral entorhinal cortex; SS2: secondary somatosensory cortex; M1: primary motor cortex; M2: secondary motor cortex; PtA: parietal association cortex

Together, these results demonstrate that *Nrg1* is mainly expressed in the MSNs of the direct pathway in the NAc.

Expression pattern of *Nrg1* in the hippocampus

The hippocampus, located beneath the cerebral cortex, is critically involved in learning and memory, in addition to spatial navigation. The hippocampus can be divided into cornu ammonis (CA) 1, 2, 3 areas, the dentate gyrus (DG), subiculum (Sub) and fasciola cinereum (FC) (Fig. 5A). The tdTomato-positive cells were mainly distributed in the DG and Sub but were very sparse in the CA and FC (Fig. 5B, C). In addition, we observed axon fiber-like tdTomato signals in the CA3 region which resemble the mossy fiber from DG granule cells (Fig. 5B). These results suggest that *Nrg1* is mostly expressed in the DG and Sub of mouse hippocampus.

To solidify the expression of *Nrg1* in the DG and Sub of adult mouse hippocampus, we performed stereotaxic injection of Cre-reporting AAV into the DG and Sub of

2-month-old *Nrg1*^{Cre/+} mice, respectively. Four weeks after AAV injection, we found tdTomato-positive cells in the DG and Sub (Fig. 5D, F), which verify the expression of *Nrg1* in the DG and Sub of adult mouse hippocampus. *Nrg1* is expressed by the mature granule neurons in the DG evidenced by the co-localization of tdTomato and NeuN, a protein marker for mature neurons (Fig. 5E). We did not observe the colocalization of tdTomato with GFAP or S100 β (two protein markers for astrocytes) in the DG (Additional file 2: Fig. S2), indicating that *Nrg1* is rarely expressed in astrocytes. In the Sub, *Nrg1* is probably expressed in the excitatory pyramidal neurons since tdTomato was co-localized with NeuN (a pan neuronal marker) but not GABA (a GABAergic neuronal marker) (Fig. 5G, H).

We further analyzed the tdTomato expression in a series of coronal sections to explore the projections of *Nrg1*-positive cells in adult mouse hippocampus. We found tdTomato expression in the cells of DG and mossy fiber of CA3

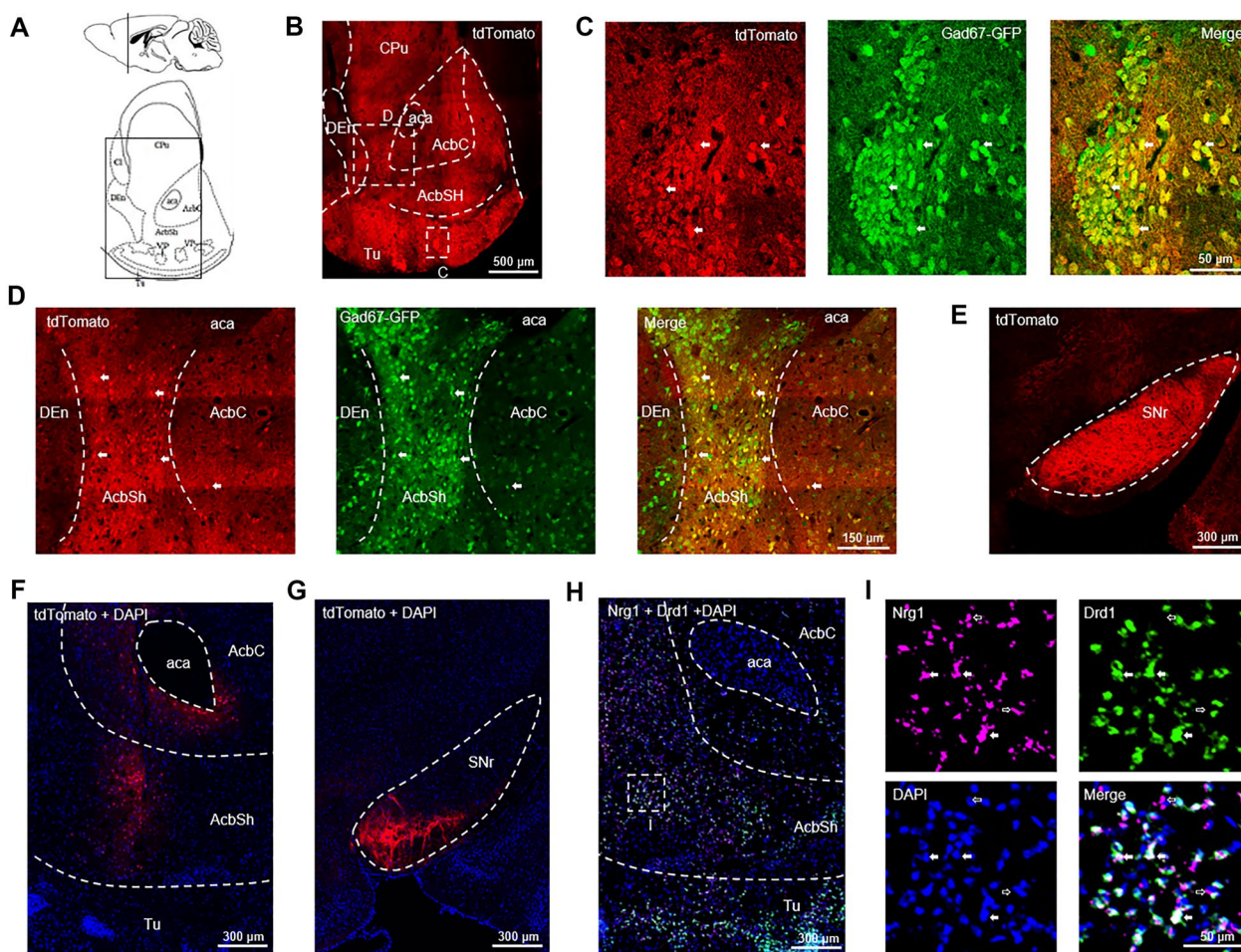


Fig. 4 Expression pattern of *Nrg1* in the striatum. **A** Diagram of mouse brain sagittal section (top) and coronal section (bottom). The line in the sagittal section diagram indicates the position of the coronal section. The rectangle indicates the brain region shown in panel B. **B** Expression of *tdTomato* in the striatum of 2-month-old *Nrg1*-reporting mice. Scale bar, 500 μ m. **C–D** Fluorescent images of *tdTomato* and *Gad67-GFP* in the Tu **C** and *AcbSH* **D** from the rectangles in panel B. Arrows indicate *Nrg1*-positive cells which are GABAergic MSNs. Scale bar, 50 μ m in panel C, 150 μ m in panel D. The *Nrg1*-reporting mice were crossed with *Gad67-GFP* transgene mice to visualize the expression of *Nrg1* in GABAergic MSNs. **E** Expression of *tdTomato* in axon fiber-like structures in the SNr. Scale bar, 300 μ m. **F–G** Expression of *tdTomato* in the NAc **F** and SNr (**G** after injection of *Cre*-reporting AAV into the NAc of 2-month-old *Nrg1^{Cre/+}* mice. Four weeks after AAV injection, the brain slices were collected and analyzed. Scale bar, 300 μ m. **H** Double fluorescence in situ hybridization (dFISH) of *Nrg1* and *Drd1* mRNA in the striatum of WT mice. Scale bar, 300 μ m. **I** The enlarged image from the rectangle in panel H. The solid arrows indicate *Nrg1*-positive cells expressing *Drd1*. The empty arrows indicate *Nrg1*-positive cells not expressing *Drd1*. Scale bar, 50 μ m. CPu: caudate putamen; Den: dorsal endopiriform nucleus; aca: anterior commissure, anterior part; AcbC: accumbens nucleus, core; AcbSH: accumbens nucleus, shell; Tu: olfactory tubercle; SNr: substantia nigra, reticular part

region (Fig. 6A). Moreover, *tdTomato* was expressed in the cells of Sub and axon fibers in the retrosplenial granular cortex (RSG), dorsal fornix (DF), fornix (F) and mammillary nucleus (MM) (Fig. 6A–C). Intriguingly, Sub pyramidal neurons send their axon projections to MM through fornix, which is part of the Papez circuit [43]. Taken together, these results demonstrate that *Nrg1* is mainly expressed in DG-CA3 pathway and Papez circuit in mouse hippocampus (Fig. 6D).

Expression pattern of *Nrg1* in the hypothalamus and thalamus

The hypothalamus is a deep structure in the brain and is localized below the thalamus (Fig. 7A). The hypothalamus is important for regulating metabolism, temperature and instinctive behaviors such as sleep, hunger, thirst, fear and maternal behaviors. In the hypothalamus of *Nrg1*-reporting mice, the *tdTomato*-positive cells were mainly distributed in the ventromedial

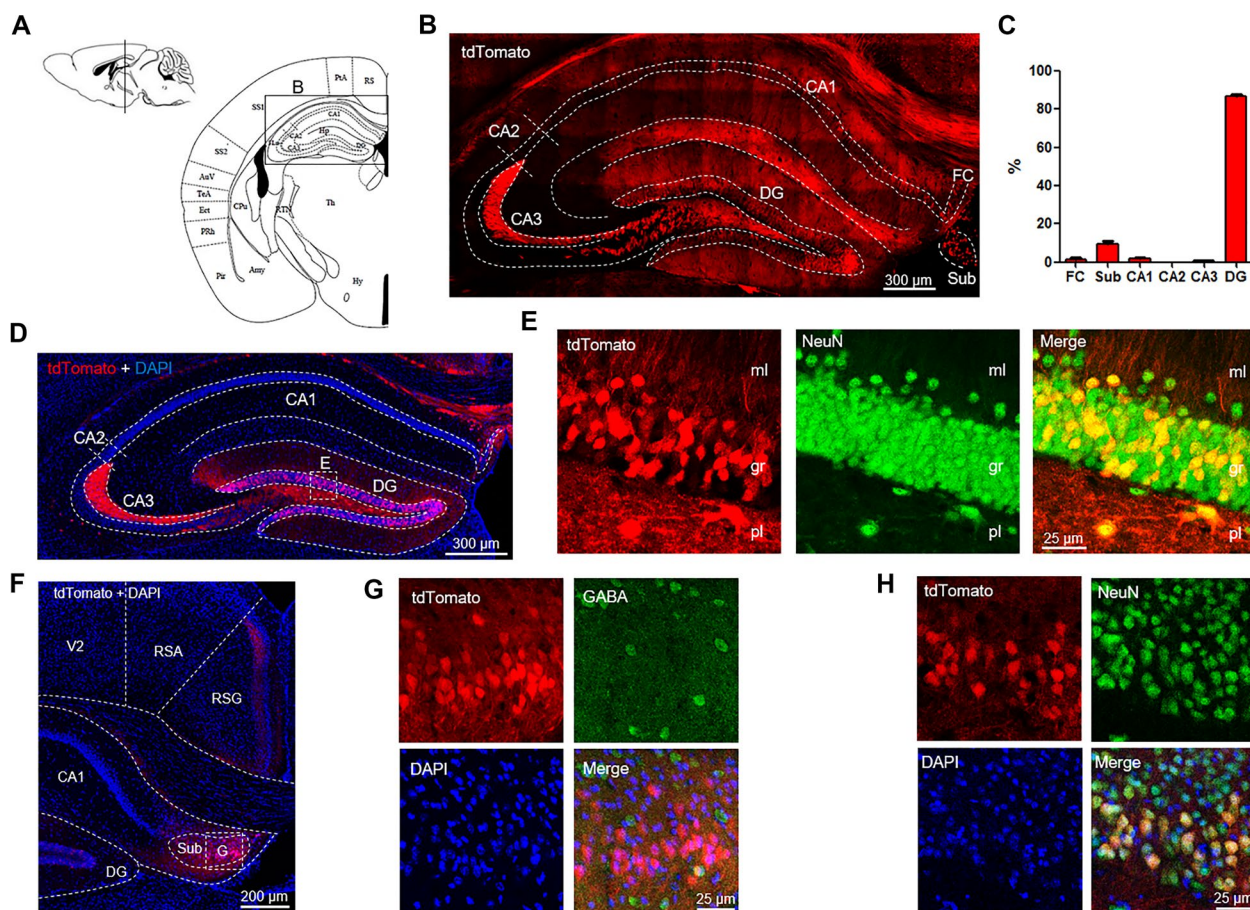


Fig. 5 Expression pattern of *Nrg1* in the hippocampus. **A** Diagram of mouse brain sagittal section (top) and coronal section (bottom). The line in the sagittal section diagram indicates the position of the coronal section. The rectangle indicates the brain region shown in panel B. **B** Expression of tdTomato in the dorsal hippocampus of 2-month-old *Nrg1*-reporting mice. Scale bar, 300 μ m. **C** The percentage of *Nrg1*-positive cells in different subregions of dorsal hippocampus among total *Nrg1*-positive cells. $P < 0.0001$, $n = 3$ mice (9 slices) for FC, $n = 6$ mice (12 slices) for other regions, one-way-ANOVA. **D** Expression of tdTomato in DG and CA3 region after injection of Cre-reporting AAV into the DG of 2-month-old *Nrg1*^{Cre/+} mice. Four weeks after AAV injection, the brain slices were collected and analyzed. Scale bar, 300 μ m. **E** Fluorescent images of tdTomato and NeuN from the rectangle in panel D. Scale bar, 25 μ m. **F** Expression of tdTomato in Sub and RS region after injection of Cre-reporting AAV into the Sub of 2-month-old *Nrg1*^{Cre/+} mice. Four weeks after AAV injection, the brain slices were collected and analyzed. Scale bar, 200 μ m. **G** Fluorescent images of tdTomato and GABA from the rectangle in panel F. Scale bar, 25 μ m. **H** Fluorescent images of tdTomato, NeuN and DAPI in the Sub of hippocampus. Scale bar, 25 μ m. FC: fasciola cinereum; Sub: subiculum; CA1: cornu ammonis 1; CA2: cornu ammonis 2; CA3: cornu ammonis 3; DG: dentate gyrus; ml: molecular layer; gr: granular layer; pl: polymorph layer; RSA: retrosplenial agranular cortex; RSG: retrosplenial granular cortex; V2: secondary visual cortex

nucleus (VM), arcuate nucleus (ARC) and median eminence (ME) (Fig. 7B). These results suggest that *Nrg1* is mostly expressed in the VM, Arc and ME of mouse hypothalamus. We also crossed *Nrg1*-reporting mice with *Gad67*-GFP mice to see whether *Nrg1* was expressed in GABAergic interneurons. In the VM, *Nrg1* is expressed in putative excitatory neurons as tdTomato is co-localized with NeuN (a pan neuronal marker) but not GFP (Fig. 7C).

The ARC contains both NPY/AgRP neurons, which are inhibited by insulin and leptin and, when activated, stimulated food intake, and POMC neurons, which

reduce food intake and are stimulated by insulin and leptin [44]. NPY/AgRP neurons can inhibit POMC neurons via synaptic release of GABA [45]. Interestingly, about two-third of tdTomato-positive cells are GABAergic in the ARC (Fig. 7D), indicating this population of *Nrg1*-positive cells are probably AgRP neurons. The tdTomato signal is highly co-localized with GFP in the ME (Fig. 7E), a region that serves as the gateway for release of hypothalamic hormones [46]. In the thalamus, the tdTomato-positive cells are mainly distributed in the superior colliculus (SC) (Fig. 7F, G), a structure that is involved in coordinating eye and head

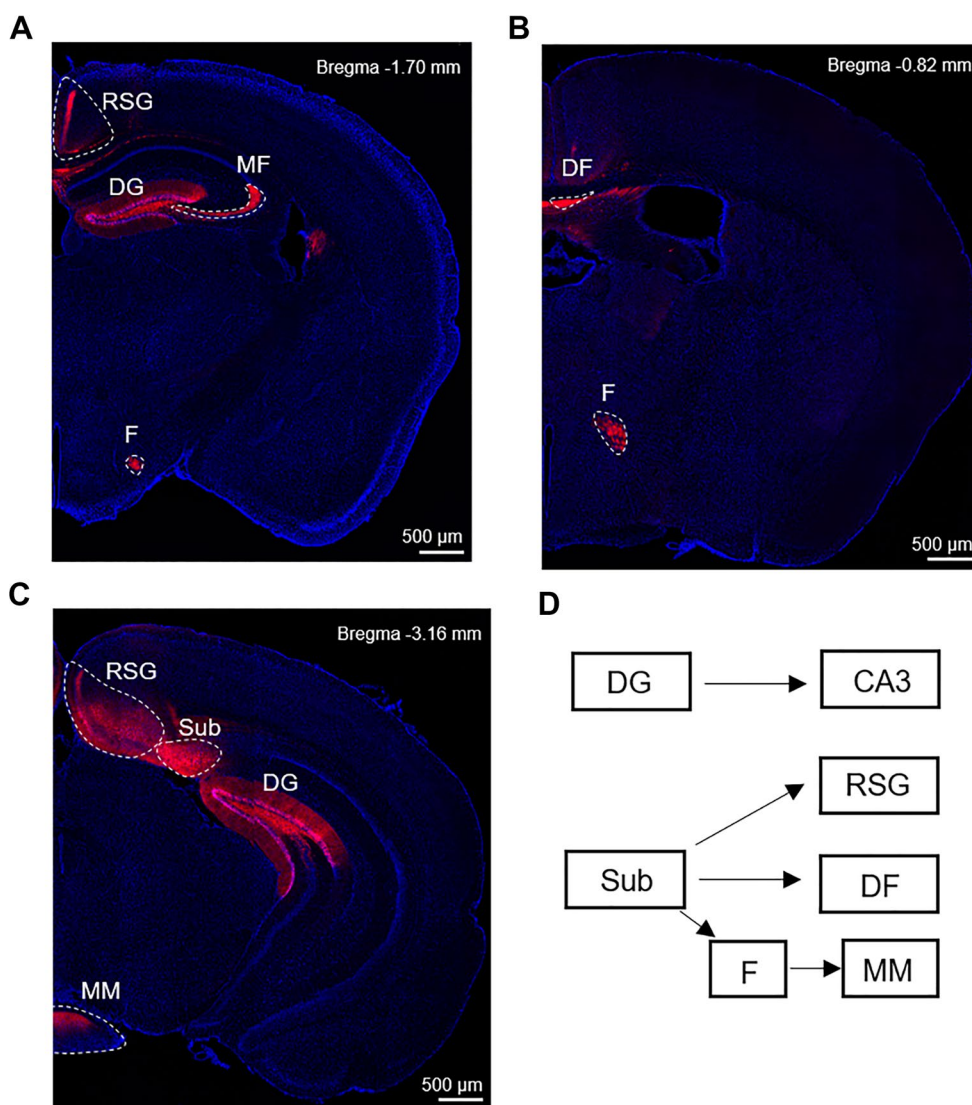


Fig. 6 Axon projections of Nrg1-positive neurons in the hippocampus. **A–C** Expression of tdTomato in coronal brain slices at the positions of bregma – 1.7 mm **A**, – 0.82 mm **B** and – 3.16 mm **C** after injection of Cre-reporting AAV into the DG and Sub of 2-month-old Nrg1^{Cre/+} mice. Four weeks after AAV injection, the brain slices were collected and analyzed. Scale bar, 500 μm. **D** Summary of the projections of Nrg1-positive neurons in the DG and Sub of mouse hippocampus. DG: dentate gyrus; RSG: retrosplenial granular cortex; MF: mossy fiber; F: fornix; DF: dorsal fornix; Sub: subiculum; MM: mammillary nucleus

movements [47]. These results suggest that Nrg1 is highly expressed in the SC of mouse thalamus. Intriguingly, nearly all tdTomato-positive cells in the SC express GFP but not vice versa (Fig. 7H). These results suggest that Nrg1 is mostly expressed in GABAergic interneurons, but not all GABAergic interneurons express Nrg1 in the mouse SC.

Expression pattern of Nrg1 in the cerebellum

The cerebellum plays important roles in motor control, emotion and cognitive functions such as attention and language. The cerebellar cortex is divided into three

layers. At the bottom lies the thick granular layer (GL), densely packed with granule cells, along with interneurons. In the middle lies the Purkinje layer (PL), a narrow zone that contains the cell bodies of Purkinje cells and Bergmann glia (BG) cells. At the top lies the molecular layer (ML), which contains the dendritic trees of Purkinje cells, along with two types of GABAergic interneurons: stellate cells and basket cells.

In the Nrg1-reporting mice, we found that tdTomato is mainly expressed in the PL and ML, but absent in the GL (Fig. 8A, B). We crossed the Nrg1-reporting mice with Gad67-GFP mice to study whether Nrg1 is

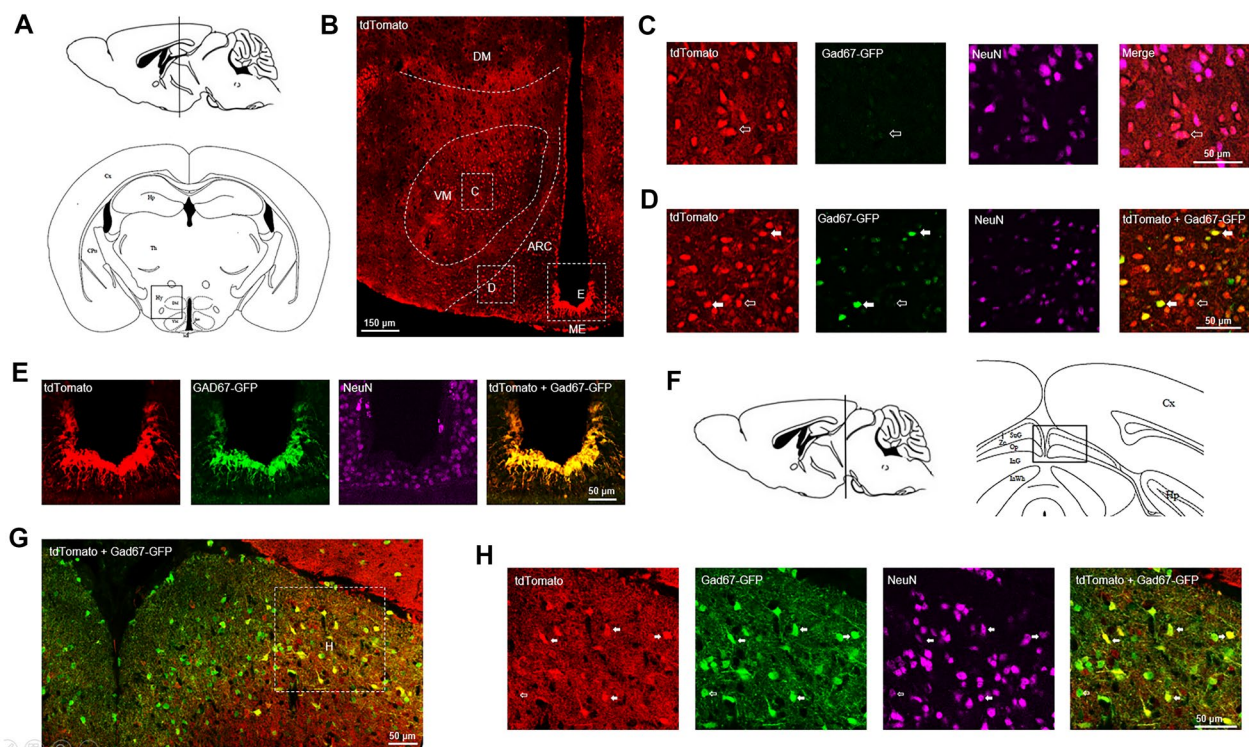


Fig. 7 Expression pattern of *Nrg1* in the hypothalamus and thalamus. **A** Diagram of mouse brain sagittal section (top) and coronal section (bottom). The line in the sagittal section diagram indicates the position of the coronal section. The rectangle indicates the brain region shown in panel B. **B** Expression of tdTomato in the hypothalamus of 2-month-old *Nrg1*-reporting mice. Scale bar, 150 μm . **C–E** Fluorescent images of tdTomato, Gad67-GFP and NeuN in the VM **C**, ARC **D** and ME **E** from the rectangles in panel B. The solid arrows indicate *Nrg1*-positive cells which are GABAergic. The empty arrows indicate *Nrg1*-positive cells not expressing Gad67-GFP. Scale bars, 50 μm . The *Nrg1*-reporting mice were crossed with Gad67-GFP mice to visualize the expression of *Nrg1* in GABAergic neurons. **F** Diagram of mouse brain sagittal section (left) and coronal section (right). The line in the sagittal section diagram indicates the position of the coronal section. The rectangle indicates the brain region shown in panel G. **G** Expression of tdTomato and Gad67-GFP in the SC of thalamus from 2-month-old *Nrg1*-reporting mice. Scale bar, 50 μm . **H** Fluorescent images of tdTomato, Gad67-GFP and NeuN from the rectangle in panel G. The solid arrows indicate GABAergic neurons expressing *Nrg1*. The empty arrow indicates GABAergic neurons not expressing *Nrg1*. Scale bar, 50 μm . DM: dorsomedial nucleus; VM: ventromedial nucleus; ARC: arcuate nucleus; ME: median eminence

expressed in the GABAergic interneurons. The tdTomato proteins were mainly expressed in the cell body of Purkinje cells in the PL, as well as in the dendritic trees of Purkinje cells and some GABAergic interneurons in the ML (Fig. 8C). Although NeuN is present in most neuronal cell types, it is not expressed in Purkinje cells (Fig. 8C), consistent with previous findings [48]. To verify that *Nrg1* is expressed in the Purkinje cells in adult mice, we injected Cre-reporting AAV into the PL of cerebellum in 2-month-old *Nrg1*^{Cre/+} mice (Fig. 8D). As shown in Fig. 8E, the tdTomato proteins were expressed in the cell bodies and dendritic trees of Purkinje cells, indicated by the co-localization of tdTomato with parvalbumin (PV), a protein marker for Purkinje cells. These results solidify the finding from *Nrg1*-reporting mice that *Nrg1* is indeed expressed in the Purkinje cells of adult mice.

Discussion

In this paper, we generated *Nrg1*-reporting mice using the cre-loxp strategy to investigate the cellular expression pattern of *Nrg1* in mouse brain. Meanwhile we revealed the axon projections of *Nrg1*-positive neurons in the mouse basal ganglion and hippocampus. These results provide fundamental information needed for understanding the function of NRG1 at the cellular and circuit levels. Here, we discuss the findings revealed by *Nrg1*-reporting mice and their relevance to physiology and brain disorders.

The results from *Nrg1*-reporting mice indicated that *Nrg1* was highly expressed in the granule cells of mouse OB. These findings are consistent with the previous study showing *Nrg1* expression in the developing mouse OB [49]. The reciprocal dendro-dendritic synapses formed

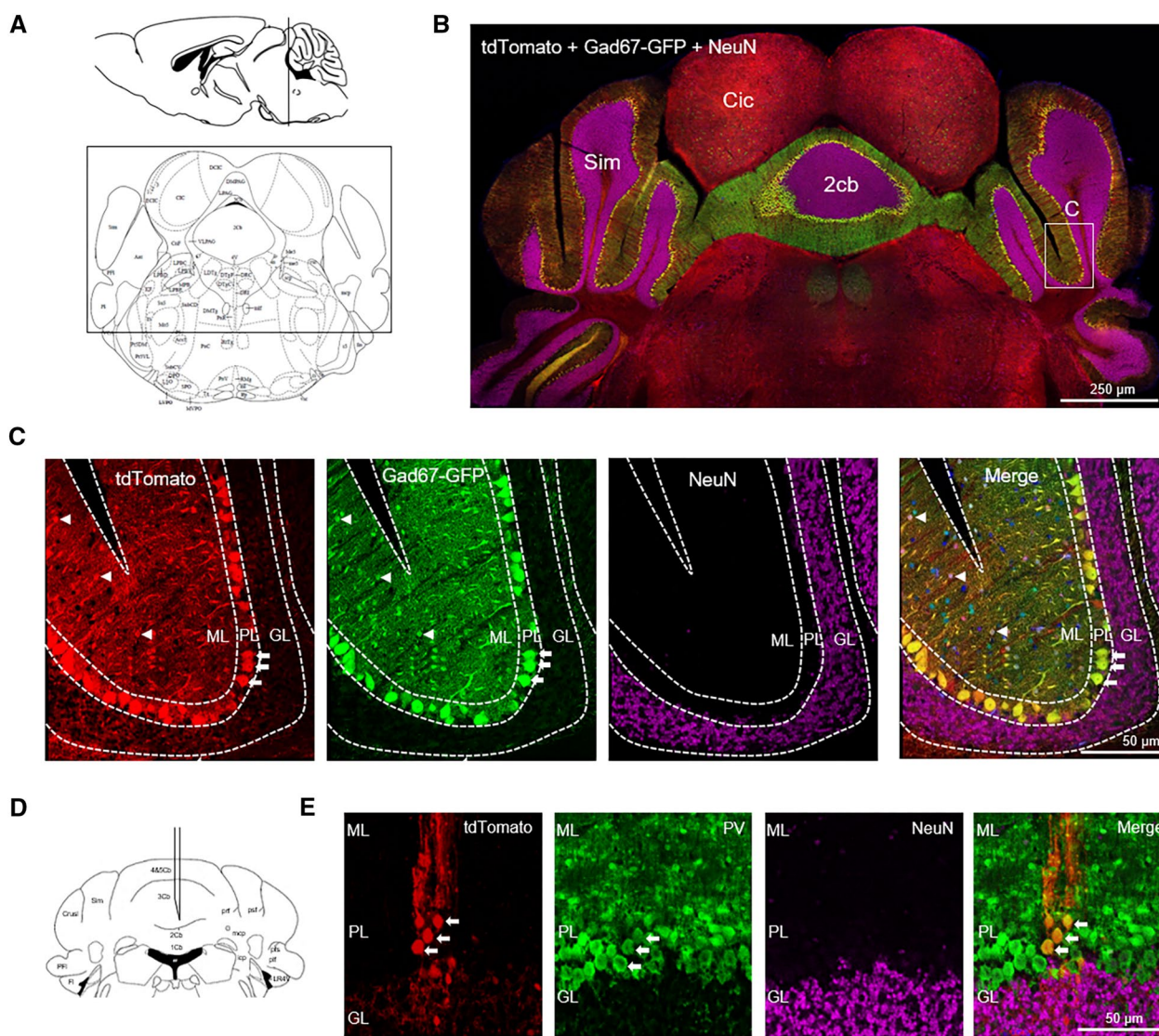


Fig. 8 Expression pattern of *Nrg1* in the cerebellum. **A** Diagram of mouse brain sagittal section (top) and coronal section (bottom). The line in the sagittal section diagram indicates the position of the coronal section. The rectangle indicates the brain region shown in panel B. **B** Fluorescent images of tdTomato, Gad67-GFP and NeuN in the cerebellum of 2-month-old *Nrg1*-reporting mice. Scale bar, 250 μ m. **C** Fluorescent images of tdTomato, Gad67-GFP and NeuN in three layers of cerebellar cortex from the rectangle in panel B. The arrows indicate the *Nrg1*-positive Purkinje cells, and the arrowheads indicate the *Nrg1*-expressing GABAergic interneurons. Scale bar, 50 μ m. The *Nrg1*-reporting mice were crossed with Gad67-GFP mice to visualize the expression of *Nrg1* in GABAergic interneurons. **D** Diagram showing the stereotaxic injection of Cre-reporting AAV into the PL of 2-month-old *Nrg1*^{Cre/+} mice. Four weeks after AAV injection, the brain slices were collected and analyzed. **E** Immunofluorescent images of tdTomato and PV in the PL of SC of *Nrg1*^{Cre/+} mice. The arrows indicate Purkinje cells expressing *Nrg1* in adult mouse cerebellum. Scale bar, 50 μ m. Sim: simple lobule; Cic: commissure of the inferior colliculus; 2cb: 2nd cerebellar lobule; GL: granular layer; PL: Purkinje layer; ML: molecular layer; PV: parvalbumin

between mitral and granule cells are considered to be important for the synchronization of mitral cells, affecting the ability of odor discrimination [50]. Intriguingly, a recent study indicated that the ErbB4 receptor of NRG1 is selectively expressed in the GABAergic interneurons in the GL and GCL of OB and regulates the ability of odor discrimination in mice [51]. NRG1-ErbB4 has been implicated in regulating synapse formation or

function through a cell-adhesion and diffusion manner, respectively [12, 14, 18, 52]. Future works are warranted to study the role of NRG1-ErbB4 signaling in the formation and function of synapse between mitral and granule cell, and whether disruption of NRG1-ErbB4 signaling in the OB causes olfactory dysfunction that is commonly observed in schizophrenia patients [53].

The data from Nrg1-reporting mice revealed that Nrg1 was mainly expressed in the layer 2–3 of cerebral cortex. By contrast, a previous study using *in situ* hybridization showed that type I/II Nrg1 mRNA was mainly expressed in layer 2–3 while type III Nrg1 mRNA was mostly expressed in layer 5 of mouse cerebral cortex [14]. These discrepancies could be due to the different sensitivity to reflect the expression of different Nrg1 splicing isoforms between the methods of genetic reporter and *in situ* hybridization. The pyramidal neurons in the layer 2–3 of cerebral cortex are responsible for the communication between different cortical regions [54, 55]. Future work is required to investigate the function of Nrg1 in regulating the crosstalk between different cortical regions.

Here we showed that Nrg1 was highly expressed in the Drd1-positive MSNs of mouse striatum, which is consistent with the single-cell RNA sequencing results from mouse striatum [29]. We further showed that Nrg1-positive neurons in the NAc send their axon projections to the SNr and thus were in the direct pathway of basal ganglion. Interestingly, the ErbB4 receptor is expressed in the dopaminergic neurons in the SNr [31, 56]. The dysfunction of the direct pathway in the basal ganglion leads to deficits in locomotion and sociability [57, 58]. Future study is warranted to investigate how the dysregulation of NRG1-ErbB4 signaling in the NAc would affect the balance between direct and indirect pathway in the basal ganglion.

The expression of Nrg1 in the DG of mouse hippocampus has been reported by previous studies [14, 59], which is in line with our findings in the Nrg1-reporting mice. Although previous studies showed moderate expression of Nrg1 in the CA1-3 pyramidal neurons [14, 26], the results from Nrg1-reporting mice indicate sparse expression of Nrg1 in the CA1-3 regions of hippocampus. By contrast, we showed here that Nrg1 is highly expressed in the subiculum, the major output region of hippocampus. The subiculum has projections to many cortical and subcortical regions. Here we showed that Nrg1-positive neurons in the subiculum send axon projections to RSG where the ErbB4 receptor is also highly expressed [31]. Moreover, Nrg1-positive neurons in the subiculum also have projections to the mammillary nucleus through fornix, which belongs to the Papez circuit [43]. It will be interesting to study the function of Nrg1 in the Papez circuit that plays important roles in the regulation of emotion [60, 61]. The data from Nrg1-reporting mice indicated that Nrg1 was mainly expressed in neurons but not astrocytes in the hippocampus under basal conditions. However, it is possible that Nrg1 can be expressed in reactive astrocytes *in vivo* or primary cultured astrocytes *in vitro* [26, 27].

The functions of Nrg1 in the thalamus and hypothalamus are relatively less well understood compared to cerebral cortex and hippocampus. The finding here that Nrg1 is highly expressed in the SC subregion of thalamus raises a possibility for Nrg1 in regulating coordination between visual stimulation and movement. We found here that Nrg1 is highly expressed in the ARC of hypothalamus. The ARC has no blood–brain barrier and can be directly affected by the circulating hormones such as insulin and leptin. Our results indicate that Nrg1 might be expressed in both the NPY/AgRP neurons and POMC neurons. Both types of neurons in the ARC project to adjacent paraventricular nucleus (PVN) to reduce food intake. Intriguingly, the ErbB4 receptor of NRG1 is highly expressed in the PVN of hypothalamus [31]. These results suggest the possibility that NRG1-ErbB4 signaling might regulate food intake through the ARC-PVH circuit. Nrg1 is also highly expressed in the GABAergic interneurons of ME, which raises a possibility that Nrg1 may regulate the release of hypothalamus hormones.

Here we found that Nrg1 is strongly expressed in the Purkinje cells in the PL of cerebellum. By contrast, the ErbB4 receptor of NRG1 is not expressed in the PL of cerebellum [31]. However, the ErbB3 receptor is highly expressed in the Bergmann glia cells in the PL and important for BG development and cerebellar lamination [62]. These results indicate that NRG1-ErbB3 signaling might regulate the maturation of BG cells. Nrg1 is also expressed in the GABAergic interneurons in the GL of cerebellum. In contrast, the ErbB4 receptor is expressed in a few glia cells but not GABAergic interneurons in the GL [31]. Future studies are warranted to investigate the role of Nrg1 in regulating the cerebellum functions.

Conclusion

Nrg1 is broadly expressed in mouse brain, mainly in neurons, but has unique expression patterns in different brain regions. The Nrg1-expressing neurons are highly presented in the direct pathway of basal ganglia, the DG to CA3 pathway and the Papez circuit. The data presented here may provide fundamental information for the study of the functions of Nrg1 and the related neural circuits in the future.

Abbreviations

Nrg1	Neuregulin 1
AAV	Adeno-associated virus
OB	Olfactory bulb
PG	Periglomerular
NAc	Nucleus accumbens
SNr	Substantia nigra pars reticulata
RSG	Retrosplenial granular cortex
MM	Mammillary nucleus

ECD	Extracellular domain
ICD	Intracellular domain
LTP	Long-term potentiation
LIMK1	LIM kinase 1
FISH	Fluorescence in situ hybridization
TRAP	Translating ribosome affinity purification
WT	Wild type
ONL	Olfactory nerve layer
GL	Glomerular layer
EPL	External plexiform layer
ML	Mitral layer
IPL	Internal plexiform layer
GCL	Granular cell layer
RMS	Rostral migratory stream
Cg1	Cingulate cortex, area 1
RS	Retrosplenial cortex
Pir	Piriform cortex
Au	Auditory cortex
M1	Primary motor cortex
M2	Secondary motor cortex
SS1	Primary somatosensory cortex
SS2	Secondary somatosensory cortex
LE	Lateral entorhinal cortex
PrL	Prelimbic cortex
CPu	Caudate putamen
MSN	Medium spiny neurons
SN	Substantia nigra
Tu	Olfactory tubercle
Drd1	Dopamine D1 receptor
Drd2	Dopamine D2 receptor
GPe	External globus pallidus
CA	Cornu ammonis
DG	Dentate gyrus
Sub	Subiculum
FC	Fasciola cinereum
GFAP	Glial fibrillary acidic protein
DF	Dorsal fornix
F	Fornix
MM	Mammillary nucleus
DM	Dorsomedial nucleus
VM	Ventromedial nucleus
ARC	Arcuate nucleus
ME	Median eminence
AgRP	Agouti-related protein
NPY	Neuropeptide Y
POMC	Pro-opiomelanocortin
SC	Superior colliculus
Sim	Simple lobule
Cic	Commissure of the inferior colliculus
2cb	2Nd cerebellar lobule
GL	Granular layer
PL	Purkinje layer
ML	Molecular layer
PV	Parvalbumin
BG	Bergmann glia

Supplementary Information

The online version contains supplementary material available at <https://doi.org/10.1186/s13578-023-01032-4>.

Additional file 1: Figure S1. The densities of Nrg1-positive cells in different brain regions of adult Nrg1-reporting mice. $n = 3$.

Additional file 2: Figure S2. Nrg1 is not expressed in astrocytes in adult mouse hippocampus. The dentate gyrus of Nrg1-reporting mice were subjected to immunostaining with anti-GFAP or anti-S100 β antibodies. Scale bar, 25 μ m.

Acknowledgements

We thank Dr. Yan-Bing Zhu from Capital Medical University for helping with the FISH experiments.

Author contributions

C-YD: conceptualization, methodology, writing—original draft; Y-TD: visualization, investigation; Y-YW: investigation, formal analysis; HJ: investigation, data curation; XZ: supervision, writing—review & editing; D-MY: supervision, resources, writing—review & editing. All authors read and approved the final manuscript.

Funding

This research was funded by National Key Research and Development Program of China (2021ZD020250), Grants from National Natural Science (No. 31861143033), the Fundamental Research Funds for the Central Universities.

Availability of data and materials

All data generated during this study are included in this published article. All unique materials used in this study are available from the corresponding author on reasonable request.

Declarations

Ethics approval and consent to participate

This study and included experimental procedures were approved by the institutional animal care and use committee of East China Normal University. All animal housing and experiments were conducted in strict accordance with the institutional guidelines for care and use of laboratory animals.

Consent for publication

Not applicable.

Competing interests

The authors declare no competing interests.

Author details

¹Key Laboratory of Brain Functional Genomics, Ministry of Education and Shanghai, School of Life Science, East China Normal University, Shanghai 200062, China. ²Center of Implant Dentistry, School and Hospital of Stomatology, Liaoning Provincial Key Laboratory of Oral Diseases, China Medical University, Shenyang 110002, China. ³Shanghai Changning Mental Health Center, Affiliated to East China Normal University, Shanghai 200335, China. ⁴Laboratory Animal Centre, China Medical University, Shenyang 110001, China. ⁵NYU-ECNU Institute of Brain and Cognitive Science at NYU Shanghai, Shanghai 200062, China.

Received: 20 February 2023 Accepted: 15 April 2023

Published online: 05 May 2023

References

- Kato T. Molecular genetics of bipolar disorder and depression. *Psychiatry Clin Neurosci*. 2007;61(1):3–19.
- Stefansson H, Sigurdsson E, Steinthorsdottir V, Bjornsdottir S, Sigmundsson T, Ghosh S, Brynjolfsson J, Gunnarsdottir S, Ivarsson O, Chou TT, et al. Neuregulin 1 and susceptibility to schizophrenia. *Am J Hum Genet*. 2002;71(4):877–92.
- Yang JZ, Si TM, Ruan Y, Ling YS, Han YH, Wang XL, Zhou M, Zhang HY, Kong QM, Liu C, et al. Association study of neuregulin 1 gene with schizophrenia. *Mol Psychiatry*. 2003;8(7):706–9.
- Mei L, Nave K-A. Neuregulin-ERBB signaling in the nervous system and neuropsychiatric diseases. *Neuron*. 2014;83(1):27–49.
- Xu Z, Jiang J, Ford G, Ford BD. Neuregulin-1 is neuroprotective and attenuates inflammatory responses induced by ischemic stroke. *Biochem Biophys Res Commun*. 2004;322(2):440–6.

6. Tan G-H, Liu Y-Y, Hu X-L, Yin D-M, Mei L, Xiong Z-Q. Neuregulin 1 represses limbic epileptogenesis through ErbB4 in parvalbumin-expressing interneurons. *Nat Neurosci*. 2011;15(2):258–66.
7. Ryu J, Hong BH, Kim YJ, Yang EJ, Choi M, Kim H, Ahn S, Baik TK, Woo RS, Kim HS. Neuregulin-1 attenuates cognitive function impairments in a transgenic mouse model of Alzheimer's disease. *Cell Death Dis*. 2016;7(2):e2117.
8. Li K-X, Lu Y-M, Xu Z-H, Zhang J, Zhu J-M, Zhang J-M, Cao S-X, Chen X-J, Chen Z, Luo J-H, et al. Neuregulin 1 regulates excitability of fast-spiking neurons through Kv11 and acts in epilepsy. *Nat Neurosci*. 2011;15(2):267–73.
9. Mei L, Xiong W-C. Neuregulin 1 in neural development, synaptic plasticity and schizophrenia. *Nat Rev Neurosci*. 2008;9(6):437–52.
10. Brinkmann BG, Agarwal A, Sereda MW, Garratt AN, Müller T, Wende H, Stassart RM, Nawaz S, Humml C, Velanac V, et al. Neuregulin-1/ErbB signaling serves distinct functions in myelination of the peripheral and central nervous system. *Neuron*. 2008;59(4):581–95.
11. Del Pino I, García-Frigola C, Dehorter N, Brotons-Mas JR, Alvarez-Salvado E, Martínez de Lagrán M, Ciceri G, Gabaldón MV, Moratal D, Dierssen M, et al. ErbB4 deletion from fast-spiking interneurons causes schizophrenia-like phenotypes. *Neuron*. 2013;79(6):1152–68.
12. Fazzari P, Paternain AV, Valiente M, Pla R, Luján R, Lloyd K, Lerma J, Marín O, Rico B. Control of cortical GABA circuitry development by Nrg1 and ErbB4 signalling. *Nature*. 2010;464(7293):1376–80.
13. Ting AK, Chen Y, Wen L, Yin D-M, Shen C, Tao Y, Liu X, Xiong W-C, Mei L. Neuregulin 1 promotes excitatory synapse development and function in GABAergic interneurons. *J Neurosci*. 2011;31(1):15–25.
14. Woo R-S, Li X-M, Tao Y, Carpenter-Hyland E, Huang YZ, Weber J, Neiswender H, Dong X-P, Wu J, Gassmann M, et al. Neuregulin-1 enhances depolarization-induced GABA release. *Neuron*. 2007;54(4):599–610.
15. Wen L, Lu Y-S, Zhu X-H, Li X-M, Woo R-S, Chen Y-J, Yin D-M, Lai C, Terry AV, Vazdarjanova A, et al. Neuregulin 1 regulates pyramidal neuron activity via ErbB4 in parvalbumin-positive interneurons. *Proc Natl Acad Sci U S A*. 2010;107(3):1211–6.
16. Chen Y-J, Zhang M, Yin D-M, Wen L, Ting A, Wang P, Lu Y-S, Zhu X-H, Li S-J, Wu C-Y, et al. ErbB4 in parvalbumin-positive interneurons is critical for neuregulin 1 regulation of long-term potentiation. *Proc Natl Acad Sci U S A*. 2010;107(50):21818–23.
17. Tan Z, Robinson HL, Yin DM, Liu Y, Liu F, Wang H, Lin TW, Xing G, Gan L, Xiong WC, et al. Dynamic ErbB4 activity in hippocampal-prefrontal synchrony and top-down attention in rodents. *Neuron*. 2018;98(2):380–93.
18. Huang YZ, Won S, Ali DW, Wang Q, Tanowitz M, Du QS, Pelkey KA, Yang DJ, Xiong WC, Salter MW, et al. Regulation of neuregulin signaling by PSD-95 interacting with ErbB4 at CNS synapses. *Neuron*. 2000;26(2):443–55.
19. Chen P, Jing H, Xiong M, Zhang Q, Lin D, Ren D, Wang S, Yin D, Chen Y, Zhou T, et al. Spine impairment in mice high-expressing neuregulin 1 due to LIMK1 activation. *Cell Death Dis*. 2021;12(4):403.
20. Wang Y-Y, Zhao B, Wu M-M, Zheng X-L, Lin L, Yin D-M. Overexpression of neuregulin 1 in GABAergic interneurons results in reversible cortical disinhibition. *Nat Commun*. 2021;12(1):278.
21. Wang JY, Miller SJ, Falls DL. The N-terminal region of neuregulin isoforms determines the accumulation of cell surface and released neuregulin ectodomain. *J Biol Chem*. 2001;276(4):2841–51.
22. Yin D-M, Chen Y-J, Lu Y-S, Bean JC, Sathyamurthy A, Shen C, Liu X, Lin TW, Smith CA, Xiong W-C, et al. Reversal of behavioral deficits and synaptic dysfunction in mice overexpressing neuregulin 1. *Neuron*. 2013;78(4):644–57.
23. Bao J, Wolpowitz D, Role LW, Talmage DA. Back signaling by the Nrg-1 intracellular domain. *J Cell Biol*. 2003;161(6):1133–41.
24. Bao J, Lin H, Ouyang Y, Lei D, Osman A, Kim T-W, Mei L, Dai P, Ohlemiller KK, Ambron RT. Activity-dependent transcription regulation of PSD-95 by neuregulin-1 and Eos. *Nat Neurosci*. 2004;7(11):1250–8.
25. Navarro-González C, Huerga-Gómez A, Fazzari P. Nrg1 intracellular signaling is neuroprotective upon stroke. *Oxid Med Cell Longev*. 2019;2019:3930186.
26. Kerber G, Streif R, Schwaiger F-W, Kreutzberg GW, Hager G. Neuregulin-1 isoforms are differentially expressed in the intact and regenerating adult rat nervous system. *J Mol Neurosci*. 2003;21(2):149–65.
27. Liu X, Bates R, Yin D-M, Shen C, Wang F, Su N, Kirov SA, Luo Y, Wang J-Z, Xiong W-C, et al. Specific regulation of NRG1 isoform expression by neuronal activity. *J Neurosci*. 2011;31(23):8491–501.
28. Sun Y, Ikrar T, Davis MF, Gong N, Zheng X, Luo ZD, Lai C, Mei L, Holmes TC, Gandhi SP, et al. Neuregulin-1/ErbB4 signaling regulates visual cortical plasticity. *Neuron*. 2016;92(1):160–73.
29. Saunders A, Macosko EZ, Wysoker A, Goldman M, Krienen FM, de Rivera H, Bien E, Baum M, Bortolin L, Wang S, et al. Molecular diversity and specializations among the cells of the adult mouse brain. *Cell*. 2018. <https://doi.org/10.1016/j.cell.2018.07.028>.
30. Vullhorst D, Neddens J, Karavanova I, Tricoire L, Petralia RS, McBain CJ, Buonanno A. Selective expression of ErbB4 in interneurons, but not pyramidal cells, of the rodent hippocampus. *J Neurosci*. 2009;29(39):12255–64.
31. Bean JC, Lin TW, Sathyamurthy A, Liu F, Yin D-M, Xiong W-C, Mei L. Genetic labeling reveals novel cellular targets of schizophrenia susceptibility gene: distribution of GABA and non-GABA ErbB4-positive cells in adult mouse brain. *J Neurosci*. 2014;34(40):13549–66.
32. Agarwal A, Zhang M, Trembak-Duff I, Unterbarnscheid T, Radyushkin K, Dibaj P, Martins de Souza D, Boretius S, Brzózka MM, Steffens H, et al. Dysregulated expression of neuregulin-1 by cortical pyramidal neurons disrupts synaptic plasticity. *Cell Rep*. 2014;8(4):1130–45.
33. Navarro-Gonzalez C, Carceller H, Benito Vicente M, Serra I, Navarrete M, Domínguez-Canterla Y, Rodríguez-Prieto Á, González-Manteiga A, Fazzari P. Nrg1 haploinsufficiency alters inhibitory cortical circuits. *Neurobiol Dis*. 2021;157:105442.
34. Law AJ, Shannon Weickert C, Hyde TM, Kleinman JE, Harrison PJ. Neuregulin-1 (NRG-1) mRNA and protein in the adult human brain. *Neuroscience*. 2004;127(1):125–36.
35. Madisen L, Zwingman TA, Sunkin SM, Oh SW, Zariwala HA, Gu H, Ng LL, Palmiter RD, Hawrylycz MJ, Jones AR, et al. A robust and high-throughput Cre reporting and characterization system for the whole mouse brain. *Nat Neurosci*. 2010;13(1):133–40.
36. Yu Q, Liu Y-Z, Zhu Y-B, Wang Y-Y, Li Q, Yin D-M. Genetic labeling reveals temporal and spatial expression pattern of D2 dopamine receptor in rat forebrain. *Brain Struct Funct*. 2019;224(3):1035–49.
37. Zhang Y-Q, Lin W-P, Huang L-P, Zhao B, Zhang C-C, Yin D-M. Dopamine D2 receptor regulates cortical synaptic pruning in rodents. *Nat Commun*. 2021;12(1):6444.
38. Kim JH, Lee SR, Li LH, Park HJ, Park JH, Lee KY, Kim MK, Shin BA, Choi SY. High cleavage efficiency of a 2A peptide derived from porcine teschovirus-1 in human cell lines, zebrafish and mice. *PLoS ONE*. 2011;6(4):e18556.
39. Li D, Qiu Z, Shao Y, Chen Y, Guan Y, Liu M, Li Y, Gao N, Wang L, Lu X, et al. Heritable gene targeting in the mouse and rat using a CRISPR-Cas system. *Nat Biotechnol*. 2013;31(8):681–3.
40. Tamamaki N, Yanagawa Y, Tomioka R, Miyazaki J-I, Obata K, Kaneko T. Green fluorescent protein expression and colocalization with calretinin, parvalbumin, and somatostatin in the GAD67-GFP knock-in mouse. *J Comp Neurol*. 2003;467(1):60–79.
41. Crittenden JR, Gipson TA, Smith AC, Bowden HA, Yildirim F, Fischer KB, Yim M, Housman DE, Graybiel AM. Striatal transcriptome changes linked to drug-induced repetitive behaviors. *Eur J Neurosci*. 2021;53(8):2450–68.
42. Gerfen CR, Surmeier DJ. Modulation of striatal projection systems by dopamine. *Annu Rev Neurosci*. 2011;34:441–66.
43. Shah A, Jhavar SS, Goel A. Analysis of the anatomy of the Papez circuit and adjoining limbic system by fiber dissection techniques. *J Clin Neurosci*. 2012;19(2):289–98.
44. Morton GJ, Cummings DE, Baskin DG, Barsh GS, Schwartz MW. Central nervous system control of food intake and body weight. *Nature*. 2006;443(7109):289–95.
45. Cowley MA, Smart JL, Rubinstein M, Cerdan MG, Diano S, Horvath TL, Cone RD, Low MJ. Leptin activates anorexigenic POMC neurons through a neural network in the arcuate nucleus. *Nature*. 2001;411(6836):480–4.
46. Palkovits M. Neuropeptides in the hypothalamo-hypophyseal system: lateral retrochiasmatic area as a common gate for neuronal fibers towards the median eminence. *Peptides*. 1984;5(Suppl 1):35–9.
47. Gandhi NJ, Katnani HA. Motor functions of the superior colliculus. *Annu Rev Neurosci*. 2011;34:205–31.
48. Wolf HK, Buslei R, Schmidt-Kastner R, Schmidt-Kastner PK, Pietsch T, Wiestler OD, Blumcke I. NeuN: a useful neuronal marker for diagnostic histopathology. *J Histochem Cytochem*. 1996;44(10):1167–71.
49. Bovevett S, De Marchis S, Gambarotta G, Fasolo A, Perroteau I, Puche AC, Bovolenta P. Differential expression of neuregulins and their receptors

- in the olfactory bulb layers of the developing mouse. *Brain Res.* 2006;1077(1):37–47.
50. Schoppa NE. Synchronization of olfactory bulb mitral cells by precisely timed inhibitory inputs. *Neuron.* 2006;49(2):271–83.
 51. Tan Z, Liu Z, Liu Y, Liu F, Robinson H, Lin TW, Xiong WC, Mei L. An ErbB4-positive neuronal network in the olfactory bulb for olfaction. *J Neurosci.* 2022;42(34):6518–35.
 52. Krivosheya D, Tapia L, Levinson JN, Huang K, Kang Y, Hines R, Ting AK, Craig AM, Mei L, Bamji SX, et al. ErbB4-neuregulin signaling modulates synapse development and dendritic arborization through distinct mechanisms. *J Biol Chem.* 2008;283(47):32944–56.
 53. Moberg PJ, Agrin R, Gur RE, Gur RC, Turetsky BI, Doty RL. Olfactory dysfunction in schizophrenia: a qualitative and quantitative review. *Neuropsychopharmacology.* 1999;21(3):325–40.
 54. Feldmeyer D, Lübke J, Sakmann B. Efficacy and connectivity of intracolumnar pairs of layer 2/3 pyramidal cells in the barrel cortex of juvenile rats. *J Physiol.* 2006;575(Pt 2):583–602.
 55. Wozny C, Williams SR. Specificity of synaptic connectivity between layer 1 inhibitory interneurons and layer 2/3 pyramidal neurons in the rat neocortex. *Cereb Cortex.* 2011;21(8):1818–26.
 56. Zheng Y, Watakabe A, Takada M, Kakita A, Namba H, Takahashi H, Yamamori T, Nawa H. Expression of ErbB4 in substantia nigra dopamine neurons of monkeys and humans. *Prog Neuropsychopharmacol Biol Psychiatry.* 2009;33(4):701–6.
 57. Shonesy BC, Parrish WP, Haddad HK, Stephenson JR, Báldi R, Bluett RJ, Marks CR, Centanni SW, Folkes OM, Spiess K, et al. Role of striatal direct pathway 2-arachidonoylglycerol signaling in sociability and repetitive behavior. *Biol Psychiatry.* 2018;84(4):304–15.
 58. Aristieta A, Barresi M, Azizpour Lindi S, Barrière G, Courtand G, de la Crompe B, Guilhemsang L, Gauthier S, Fioramonti S, Baufretton J, et al. A disynaptic circuit in the globus pallidus controls locomotion inhibition. *Curr Biol.* 2021. <https://doi.org/10.1016/j.cub.2020.11.019>.
 59. Mahar I, Tan S, Davoli MA, Dominguez-Lopez S, Qiang C, Rachalski A, Turecki G, Mechawar N. Subchronic peripheral neuregulin-1 increases ventral hippocampal neurogenesis and induces antidepressant-like effects. *PLoS ONE.* 2011;6(10):e26610.
 60. Pessoa L, McMenamin B. Dynamic networks in the emotional brain. *Neuroscientist.* 2017;23(4):383–96.
 61. Pratt JA. The neuroanatomical basis of anxiety. *Pharmacol Ther.* 1992;55(2):149–81.
 62. Sathyamurthy A, Yin DM, Barik A, Shen C, Bean JC, Figueiredo D, She JX, Xiong WC, Mei L. ERBB3-mediated regulation of Bergmann glia proliferation in cerebellar lamination. *Development.* 2015;142(3):522–32.

Publisher's Note

Springer Nature remains neutral with regard to jurisdictional claims in published maps and institutional affiliations.

Ready to submit your research? Choose BMC and benefit from:

- fast, convenient online submission
- thorough peer review by experienced researchers in your field
- rapid publication on acceptance
- support for research data, including large and complex data types
- gold Open Access which fosters wider collaboration and increased citations
- maximum visibility for your research: over 100M website views per year

At BMC, research is always in progress.

Learn more biomedcentral.com/submissions

